



Cite this: *Environ. Sci.: Water Res. Technol.*, 2018, 4, 1219

## Emerging investigators series: comparative study of naproxen degradation by the UV/chlorine and the UV/H<sub>2</sub>O<sub>2</sub> advanced oxidation processes†

Mingwei Pan,<sup>‡</sup> Zihao Wu,<sup>‡</sup> Changyuan Tang,<sup>ab</sup> Kaiheng Guo,<sup>id</sup> Yingjie Cao<sup>a</sup> and Jingyun Fang<sup>id</sup>\*

The UV/chlorine advanced oxidation process (AOP), which forms HO<sup>•</sup> and reactive chlorine species (RCS such as Cl<sup>•</sup>, ClO<sup>•</sup> and Cl<sub>2</sub><sup>•-</sup>), is being considered as an alternative to the UV/H<sub>2</sub>O<sub>2</sub> AOP for the degradation of emerging organic contaminants. This study compared the kinetics and pathways of the degradation of a recalcitrant pharmaceutically active compound, naproxen (NPX), by the UV/chlorine and UV/H<sub>2</sub>O<sub>2</sub> AOPs. The degradation of NPX by both AOPs followed pseudo first-order kinetics, and, at pH 7, the first-order rate constant (*k*) in UV/chlorine was 4.9 times higher than that in UV/H<sub>2</sub>O<sub>2</sub>. At pH 7, in the UV/chlorine process, the HO<sup>•</sup> and RCS contributed to 15.9% and 76.3%, respectively, of the NPX degradation. Radical scavenging tests indicated that ClO<sup>•</sup> and CO<sub>3</sub><sup>•-</sup> were important to the NPX degradation by UV/chlorine. A higher efficiency was observed in UV/chlorine than in UV/H<sub>2</sub>O<sub>2</sub> at the pH range of 6–9, but as the pH rose from 6 to 9, *k* decreased from 6.10 × 10<sup>-3</sup> s<sup>-1</sup> to 2.98 × 10<sup>-3</sup> s<sup>-1</sup> in UV/chlorine. However, in UV/H<sub>2</sub>O<sub>2</sub>, *k* was only slightly affected by pH. In both AOPs, *k* increased linearly with increasing dosages of oxidants (chlorine or H<sub>2</sub>O<sub>2</sub>) from 20 μM to 200 μM. The UV/H<sub>2</sub>O<sub>2</sub> process was less affected by the water matrix than the UV/chlorine process. Compared to pure water, *k* in tap water was reduced by 9% and 23.2% by UV/H<sub>2</sub>O<sub>2</sub> and UV/chlorine, respectively. The degradation by both AOPs was associated with hydroxylation and demethylation. Decarboxylation was particularly observed in UV/H<sub>2</sub>O<sub>2</sub>, and chlorine substitution was observed in UV/chlorine. During the UV/chlorine process, the acute toxicity to *Vibrio fischeri* increased and then decreased in the system.

Received 16th February 2018,  
Accepted 13th May 2018

DOI: 10.1039/c8ew00105g

rsc.li/es-water

### Water impact

The efficiency of the UV/chlorine advanced oxidation process (AOP) for naproxen degradation is much better compared to the UV/H<sub>2</sub>O<sub>2</sub> AOP, indicating that the former can be a good alternative to the latter for the degradation of micropollutants. The transformation pathways of micropollutants by the two AOPs display similarities and differences due to the involvement of reactive chlorine species in UV/chlorine.

## 1. Introduction

The occurrence and fate of pharmaceutically active compounds (PhACs) in the aquatic environment have received considerable attention in recent years<sup>1,2</sup> due to the potential threats to humans and wildlife at low concentrations.<sup>3,4</sup>

Naproxen (NPX), one of the best-selling nonprescription drugs in the world, is a synthetic nonsteroidal anti-inflammatory drug that is commonly used as an analgesic and antipyretic. Owing to its limited removal efficiency during municipal sewage treatment processes, NPX became one of the most frequently detected PhACs in surface water.<sup>5</sup> The occurrence of NPX ranged 0.5–7.84 μg L<sup>-1</sup> in wastewaters,<sup>6</sup> 0.4–263 ng L<sup>-1</sup> in surface waters<sup>7–9</sup> and <11 ng L<sup>-1</sup> in drinking waters.<sup>1,10</sup> Most conventional water treatment processes are incapable of removing NPX effectively, such as active sludge,<sup>11</sup> activated carbon sorption (the Freundlich constant is 0.71 × 10<sup>-4</sup> at pH 6.5),<sup>12</sup> coagulation–flocculation, flotation,<sup>12</sup> and chlorination.<sup>8</sup>

The UV/H<sub>2</sub>O<sub>2</sub> advanced oxidation process (AOP) generates hydroxyl radicals (HO<sup>•</sup>) (eqn (1)), which are effective in NPX removal with a second-order rate constant of 1 × 10<sup>10</sup> M<sup>-1</sup>

<sup>a</sup> Guangdong Provincial Key Laboratory of Environmental Pollution Control and Remediation Technology, School of Environmental Science and Engineering, Sun Yat-Sen University, Guangzhou 510275, China. E-mail: fangjy3@mail.sysu.edu.cn; Tel: +86 20 8411 0692

<sup>b</sup> School of Geography and Planning, Sun Yat-Sen University, Guangzhou, 510275, China

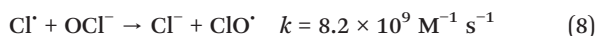
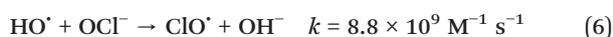
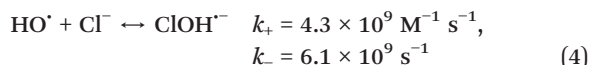
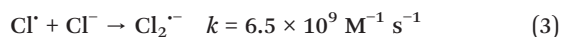
† Electronic supplementary information (ESI) available. See DOI: 10.1039/c8ew00105g

‡ Shared first authorship.

$\text{s}^{-1}$ .<sup>13,14</sup> However, the energy requirement of UV/H<sub>2</sub>O<sub>2</sub> is relatively high.<sup>15</sup> The UV/chlorine AOP can be an alternative to the UV/H<sub>2</sub>O<sub>2</sub> AOP in water treatment, which simultaneously generates non-selective HO· and selective chlorine atom (Cl·) by UV photolysis of free chlorine (HOCl/OCl<sup>-</sup>) (eqn (2)).<sup>16</sup> The formation of radicals in UV/chlorine is higher than that in UV/H<sub>2</sub>O<sub>2</sub>,<sup>17</sup> which is likely to eventually reduce the energy requirement in UV/chlorine. It has been reported that UV/chlorine saved 30–75% electrical energy per order (EE/O) for the abatement of the same amount of contaminants (such as 17 $\alpha$ -ethinylestradiol, desethylatrazine, sulfamethoxazole, carbamazepine, benzotriazole, tolyltriazole, iopamidol and diclofenac) compared to UV/H<sub>2</sub>O<sub>2</sub>.<sup>18</sup> However, the comparative efficiencies of the UV/H<sub>2</sub>O<sub>2</sub> and UV/chlorine AOPs for the degradation of NPX are unclear.



Both HO· and Cl· have been proven to be important reactive species in the UV/chlorine AOP.<sup>16,19,20</sup> In addition to the primary radicals HO· and Cl·, various secondary radicals such as ClO· and Cl<sub>2</sub><sup>-</sup> are formed in the following chain reactions in the UV/chlorine AOP (eqn (3)–(8)).<sup>16</sup>



RCS such as Cl·, ClO·, and Cl<sub>2</sub><sup>-</sup> have been reported to be more selective than HO· and prefer to attack chemicals containing electron-rich groups.<sup>16,21</sup> In particular, the role of ClO· is important for the degradation of some pollutants in the UV/chlorine AOP due to its relatively high concentrations and high reactivity with some pollutants.<sup>22–24</sup> The concentrations of ClO· have been reported to be several orders of magnitude higher than those of HO· and Cl·, and the rate constants are in the range of 10<sup>7</sup>–10<sup>9</sup> M<sup>-1</sup> s<sup>-1</sup> for carbamazepine, caffeine, gemfibrozil and dimethoxybenzenes.<sup>24</sup> However, the contributions of RCS such as Cl· and ClO· to the degradation of NPX by UV/chlorine are currently unknown. Additionally, the involvement of both HO· and RCS in the AOP makes the transformation pathways complicated, particularly since chlorine-containing products can be produced through the RCS pathway. Thus, the transformation pathway by the UV/chlorine AOP deserves investigation.

The concentrations of radicals involved in the UV/chlorine and UV/H<sub>2</sub>O<sub>2</sub> AOPs have been reported to be affected by water matrix components in real water treatment, and thus affect the degradation of pollutants.<sup>23–25</sup> pH has been reported to have a profound effect on the degradation efficiency of the UV/chlorine process,<sup>24</sup> but not the UV/H<sub>2</sub>O<sub>2</sub> process.<sup>26</sup> The degradation of most micropollutants bearing electron-withdrawing groups (such as ibuprofen, benzoic acid) decreased with increasing pH by UV/chlorine, while that for micropollutants primarily relying on ClO· (such as gemfibrozil, diclofenac, and trimethoprim) reached a maximum at pH 7.<sup>16,22,24</sup> This phenomenon can be attributed to the different pK<sub>a</sub> of HOCl (7.5) and H<sub>2</sub>O<sub>2</sub> (11.7). Increasing chlorine dosage promoted the generation of ClO·, but not HO·.<sup>23</sup> Water matrix components such as dissolved organic matter (DOM), alkalinity, ammonia and halides have been reported to differently affect the degradation of pollutants in the UV/chlorine and UV/H<sub>2</sub>O<sub>2</sub> AOPs.<sup>16,27</sup> For example, through filtering UV light and scavenging radicals,<sup>16,28,29</sup> DOM restrained the degradation of some pollutants by the UV/H<sub>2</sub>O<sub>2</sub> and UV/chlorine AOPs, while halides enhanced the efficiency of the two AOPs by forming ClBr<sup>-</sup>.<sup>23,30</sup> The studies mentioned indicate that the effects of operational factors and water matrices on the degradation of pollutants are compound specific.<sup>23,24,27</sup> Thus, the effects of the water matrix components on the degradation of NPX and its degradation in real waters should be investigated.

Thus, the aims of this work are as follows: 1) to compare the degradation kinetics of NPX by the UV/chlorine and the UV/H<sub>2</sub>O<sub>2</sub> AOPs under different conditions; 2) to reveal the underlying radical mechanism controlling the kinetics; and 3) to explore the transformation pathways and toxicity alternation by the two AOPs.

## 2. Materials and methods

### 2.1. Reagents

All solutions were prepared with reagent-grade chemicals and ultrapure water (18.2 M $\Omega$  cm) produced by a Milli-Q system (Millipore, Reference). NPX (98%) was obtained from Fluorochem (Hadfield, UK). Nitrobenzene (NB, 99%), 1,4-dimethoxybenzene (DMOB), *tert*-butanol (TBA). HPLC grade methanol, acetonitrile and *o*-phosphoric acid were obtained from Fisher Scientific. NaHCO<sub>3</sub>, NaCl, NaBr, (NH<sub>4</sub>)<sub>2</sub>SO<sub>4</sub> and NH<sub>4</sub>Cl were obtained from Sinopharm Chemical Reagent Co., Ltd. (Shanghai, China). Suwannee River natural organic matter (NOM) isolate (Cat. No. 1R101N) was obtained from the International Humic Substance Society. pH was buffered with phosphate buffer with/without sodium hydroxide.

A free chlorine stock solution (3400 mg L<sup>-1</sup> as Cl<sub>2</sub>) was prepared from 4.00–4.99% sodium hypochlorite (NaOCl) (Sigma-Aldrich) and periodically standardized by DPD/FAS titration.<sup>31</sup> A H<sub>2</sub>O<sub>2</sub> stock solution (200 mM) was prepared from 27% H<sub>2</sub>O<sub>2</sub> solution (Alfa Aesar) and periodically standardized by the I<sub>3</sub><sup>-</sup> colorimetric method.<sup>32</sup> The NOM stock solution was prepared by dissolving Suwannee River RO NOM isolate

in the ultrapure water and then filtering it through a 0.45  $\mu\text{m}$  membrane.

## 2.2. Experimental procedures

The photochemical experiments were performed in a 700 mL cylindrical photoreactor with a low pressure mercury lamp (Heraeus GPH 212T5L/4, 10 W) covered by a quartz tube in the center. The reacting solution was magnetically stirred during the reaction and the temperature was maintained at  $25(\pm 0.2)$  °C. More details about this reactor can be found in a previous study.<sup>20</sup> The UV photon flux ( $I_0$ ) entering the solution was determined to be  $0.471 \mu\text{E s}^{-1}$  using iodide/iodate chemical actinometry.<sup>33</sup> The effective path length ( $L$ ) was determined to be 2.43 cm by measuring the kinetics of the photolysis of dilute  $\text{H}_2\text{O}_2$ .<sup>34</sup>

A 700 mL testing solution containing 5  $\mu\text{M}$  NPX and 2 mM phosphate buffer (pH 7) was dosed with 50  $\mu\text{M}$  oxidant ( $\text{NaOCl}$  or  $\text{H}_2\text{O}_2$ ) and simultaneously exposed to UV light. This condition was defined as the baseline. Samples (1 mL) were collected at different time intervals and quenched with  $\text{NH}_4\text{Cl}$ . All the samples were analyzed in 24 hours. An orthogonal matrix experimental design was employed, where one parameter of oxidant dosage, pH, alkalinity, NOM, ammonium, chloride or bromide concentration was varied at a time relative to the baseline condition, as follows: oxidant dosage (25, 50, 100 and 200  $\mu\text{M}$ ), pH values (6, 7 and 9), alkalinity (1 and 3 mM  $\text{HCO}_3^-$ ), NOM (1 and 3 mg  $\text{L}^{-1}$  (as DOC)), ammonium (25, 50 and 75  $\mu\text{M}$ ), chloride (5 mM), bromide (5, 10 and 20  $\mu\text{M}$ ) and chloride (5 mM) + bromide (10  $\mu\text{M}$ ). Control tests of NPX degradation by direct UV photolysis and dark chlorination were carried out in a similar manner but in the absence of chlorine and UV irradiation, respectively. At least one data set was duplicated for quality control, in which error bars are shown in each figure. The error bars represent the maximum and minimum of the experimental data of the duplicated test results.

To determine the intermediates/products during NPX degradation by the UV/chlorine and UV/ $\text{H}_2\text{O}_2$  AOPs, higher initial concentrations of NPX (50  $\mu\text{M}$ ) and oxidant ( $\text{NaOCl}$  or  $\text{H}_2\text{O}_2$ , 200  $\mu\text{M}$ ) were used. After a certain reaction time in each run, the reaction was quenched with ammonia chloride and a 500 mL sample was collected and subjected to solid-phase extraction (SPE) pretreatment following ref. 22 for QTOF MS analyses.<sup>22</sup>

## 2.3. Analytical methods

The pH was measured with a pH metre (FE20, Mettler Toledo). Dissolved organic carbon (DOC) was measured using a total organic carbon (TOC) analyzer (TOC-V<sub>CPH</sub>, Shimadzu, Japan). The concentrations of NPX and NB were measured using high-performance liquid chromatography (HPLC, Agilent 1260, USA) equipped with a C18 column (Poroshell,  $4.6 \times 50$  mm, 2.7  $\mu\text{m}$ ) and a diode array detector (DAD) with the wavelength set at 230 nm and 266 nm, respectively. The mobile phase for the determination of NPX and NB consisted of 0.5% phospho-

ric acid solution/methanol (50:50, v/v%) and water/methanol (70:30, v/v%), respectively, at a flow rate of 1 mL  $\text{min}^{-1}$ .

The transformation products of NPX during the UV/chlorine and UV/ $\text{H}_2\text{O}_2$  AOPs were identified by an UPLC system coupled to an Ion Mobility-QTOF MS (Waters Synapt G2-Si, USA). The operating conditions of the UPLC-QTOF MS in the ESI negative mode are detailed in Text S1.

Acute toxicity tests were carried out using *Vibrio fischeri* strains and data were analyzed on a LUMISTox toxicity analyzer (HACH, USA). The results after 30 min contact periods were reported as luminescence inhibition (%). To prevent uncorrected toxicity bioassay interpretations, all the samples were diluted to give a final chloride concentration of 3%.<sup>22</sup>

## 2.4. Relative radical contribution

The kinetics of the UV/chlorine process was investigated by steady-state assumption to evaluate the individual contributions of UV, chlorination,  $\text{HO}^\bullet$ , and RCS (such as  $\text{Cl}^\bullet$ ,  $\text{ClO}^\bullet$ ,  $\text{Cl}_2^\bullet$ ) to the degradation of NPX. NB was selected as a probe compound to differentiate the contribution of  $\text{HO}^\bullet$  and RCS following the method developed by Xiang *et al.* (2016).<sup>20</sup> The rate constant of  $\text{HO}^\bullet$  with NPX degradation was reported to be  $1 \times 10^{10} \text{ M}^{-1} \text{ s}^{-1}$  at pH 7–8.<sup>35</sup>

## 2.5. Determination of the second-order rate constant of $\text{ClO}^\bullet$

The second-order rate constant of  $\text{ClO}^\bullet$  reacting with NPX was determined by competition kinetics using DMOB as a reference compound.<sup>23,24</sup> A  $\text{ClO}^\bullet$  scenario was created following the method of Wu *et al.* (2017).<sup>23</sup> NPX and DMOB were simultaneously spiked to the system at the same concentration of 5  $\mu\text{M}$ . Control experiments of direct UV photolysis or chlorination alone were carried out in a similar manner but in the absence of chlorine and UV irradiation, respectively. The calculation of the second-order rate constant of NPX with  $\text{ClO}^\bullet$  followed the method described in a previous study.<sup>23</sup>

# 3. Results and discussion

## 3.1. Degradation kinetics

Fig. 1 shows the time-dependent degradation of NPX by UV irradiation, chlorination,  $\text{H}_2\text{O}_2$ , UV/chlorine and UV/ $\text{H}_2\text{O}_2$  in pure water at pH 7. NPX was degraded by 27.3% at a UV dosage of 922  $\text{mJ cm}^{-2}$  due to the high molar absorptivity of 4024  $\text{M}^{-1} \text{ cm}^{-1}$  at 254 nm (Fig. S1†), which is consistent with a previous study.<sup>36</sup> The degradation of NPX by  $\text{H}_2\text{O}_2$  or chlorine alone was negligible. The degradation by the UV/ $\text{H}_2\text{O}_2$  and the UV/chlorine AOPs followed pseudo first-order kinetics with rate constants ( $k'$ ) of  $1.44 \times 10^{-3} \text{ s}^{-1}$  and  $7.07 \times 10^{-3} \text{ s}^{-1}$ , respectively. The greater degradation efficiency of the UV/chlorine AOP may be attributable to the relatively higher reactive radical production.<sup>16</sup> Specifically, the molar absorption coefficients of  $\text{HOCl}$ ,  $\text{OCl}^-$ , and  $\text{H}_2\text{O}_2$  at 254 nm were reported to be  $59 \pm 1$ ,  $66 \pm 1$ , and  $\sim 19 \text{ M}^{-1} \text{ cm}^{-1}$ , respectively,<sup>37,38</sup> and their quantum yields at 254 nm were 1.45, 0.97, and 0.5  $\text{mol Es}^{-1}$ , respectively.<sup>16,38</sup>

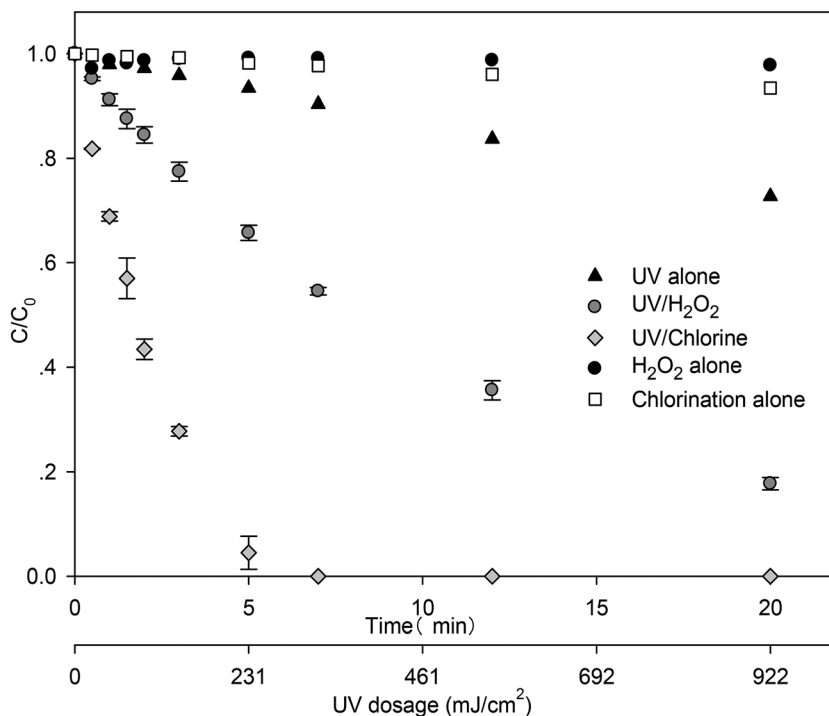


Fig. 1 Time-dependent degradation of NPX by UV irradiation, chlorination,  $\text{H}_2\text{O}_2$ , and the UV/ $\text{H}_2\text{O}_2$  and UV/chlorine AOPs in pure water at pH 7. Conditions:  $[\text{chlorine}]_0 = [\text{H}_2\text{O}_2]_0 = 50 \mu\text{M}$ ,  $[\text{NPX}]_0 = 5 \mu\text{M}$ ,  $[\text{phosphate buffer}]_0 = 2 \text{ mM}$ .

The EE/O of NPX by the UV/chlorine and UV/ $\text{H}_2\text{O}_2$  AOPs was calculated (Text S2†). At the oxidant dosage of  $50 \mu\text{M}$ , the EE/O values for 90% NPX removal by the UV/chlorine and UV/ $\text{H}_2\text{O}_2$  AOPs were  $0.153$  and  $0.578 \text{ kW h m}^{-3}$ , respectively, indicating that the UV/chlorine AOP is more efficient.

### 3.2. Radical mechanisms of NPX by the UV/chlorine and UV/ $\text{H}_2\text{O}_2$ AOPs

**3.2.1. Identification of the free radical species attributable to the NPX degradation.** Fig. 2 shows the contribution of the reactive species to NPX degradation in the UV/chlorine and the UV/ $\text{H}_2\text{O}_2$  AOPs. At pH 7, UV photolysis and  $\text{HO}^\bullet$

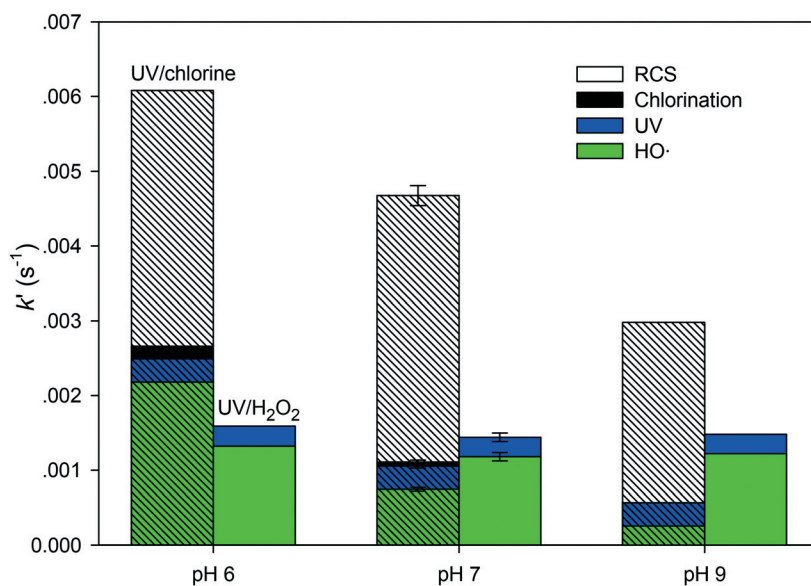


Fig. 2 Effect of pH on the  $k'$  of NPX degradation by UV irradiation, chlorination,  $\text{HO}^\bullet$ , and RCS ( $\text{Cl}^\bullet$ ,  $\text{ClO}^\bullet$ ,  $\text{Cl}_2^\bullet$ ) in the UV/chlorine and UV/ $\text{H}_2\text{O}_2$  AOPs in pure water. Conditions:  $[\text{NPX}]_0 = 5 \mu\text{M}$ ,  $[\text{chlorine}]_0 = [\text{H}_2\text{O}_2]_0 = 50 \mu\text{M}$ ,  $[\text{NB}]_0 = 1 \mu\text{M}$ ,  $[\text{phosphate buffer}]_0 = 2 \text{ mM}$ .

accounted for 19.4% and 80.6% of the  $k'$  in the UV/H<sub>2</sub>O<sub>2</sub> AOP, respectively, while UV photolysis, chlorine, HO<sup>•</sup> and RCS accounted for 6.6%, 1.2%, 15.9% and 76.3% of the  $k'$  in the UV/chlorine AOP, respectively. RCS played a dominant role in NPX degradation in the UV/chlorine AOP. The time-dependent degradation of NPX and NB in the processes is shown in Fig. S2 and S3.†

Radical scavengers of HCO<sub>3</sub><sup>-</sup> and TBA were added to the two AOPs to identify the specific contribution of radicals. The reactivities between radical scavengers of HCO<sub>3</sub><sup>-</sup> and TBA and the radicals are shown in Table S1.† HCO<sub>3</sub><sup>-</sup> significantly scavenges HO<sup>•</sup>, Cl<sup>•</sup> and Cl<sub>2</sub><sup>-•</sup> to form CO<sub>3</sub><sup>-•</sup> but scarcely scavenges ClO<sup>•</sup>, while TBA scavenges HO<sup>•</sup>, Cl<sup>•</sup> and ClO<sup>•</sup> but hardly scavenges Cl<sub>2</sub><sup>-•</sup> and CO<sub>3</sub><sup>-•</sup>.<sup>23</sup> Fig. 3 shows the effects of HCO<sub>3</sub><sup>-</sup> and TBA on the degradation of NPX by the UV/chlorine and UV/H<sub>2</sub>O<sub>2</sub> AOPs at pH 8.4. In the presence of 100 mM HCO<sub>3</sub><sup>-</sup>, HO<sup>•</sup>, Cl<sup>•</sup> and Cl<sub>2</sub><sup>-•</sup> were totally scavenged, while  $k'$  decreased by 6.5% and 23.6% in UV/chlorine and UV/H<sub>2</sub>O<sub>2</sub>, respectively. As the reaction rate constant of CO<sub>3</sub><sup>-•</sup> and NPX has been reported to be  $5.6 \times 10^7 \text{ M}^{-1} \text{ s}^{-1}$ ,<sup>13</sup> the formation of CO<sub>3</sub><sup>-•</sup> can contribute to the NPX degradation in both AOPs. Additionally, ClO<sup>•</sup>, which was less affected by HCO<sub>3</sub><sup>-</sup> ( $k = 600 \text{ M}^{-1} \text{ s}^{-1}$ ),<sup>39</sup> can be important to the NPX degradation. In the presence of 2 mM TBA, HO<sup>•</sup> was scavenged to over 90%, with the  $k'$  of NPX degradation decreasing by 35.1% and 65.9% in UV/chlorine and UV/H<sub>2</sub>O<sub>2</sub>, respectively. The larger scavenging effect of 2 mM TBA than 100 mM HCO<sub>3</sub><sup>-</sup> further indicates the contribution of ClO<sup>•</sup> in UV/chlorine and the contribution of CO<sub>3</sub><sup>-•</sup> in both AOPs. Therefore, besides HO<sup>•</sup> and Cl<sup>•</sup>, ClO<sup>•</sup> and CO<sub>3</sub><sup>-•</sup> are important to the degradation of NPX.

**3.2.2. Effect of pH on the kinetics and radical contribution.** Fig. 2 shows the  $k'$  of NPX degradation by UV, oxidants, HO<sup>•</sup> and RCS in the UV/chlorine and UV/H<sub>2</sub>O<sub>2</sub> AOPs at pH 6, 7 and 9, respectively. pH slightly affected the  $k'$  by either di-

rect UV photolysis or UV/H<sub>2</sub>O<sub>2</sub>, but the  $k'$  decreased by UV/chlorine with increasing pH. Nevertheless, the NPX degradation was more efficient by UV/chlorine compared to UV/H<sub>2</sub>O<sub>2</sub> at all pH values tested. As the pH increased from 6 to 9, the  $k'$  of the UV/chlorine AOP decreased from  $6.10 \times 10^{-3} \text{ s}^{-1}$  to  $2.98 \times 10^{-3} \text{ s}^{-1}$  where  $k'_{\text{HO}^{\bullet}}$  decreased from  $2.18 \times 10^{-3} \text{ s}^{-1}$  to  $2.56 \times 10^{-4} \text{ s}^{-1}$  and  $k'_{\text{RCS}}$  decreased from  $3.42 \times 10^{-3} \text{ s}^{-1}$  to  $2.41 \times 10^{-3} \text{ s}^{-1}$ . As the proportion of HOCl is relatively higher (Table S2†) and the quantum yield of chlorine decay at 254 nm is higher for HOCl (1.45 mol Es<sup>-1</sup>) than OCl<sup>-</sup> (0.97 mol Es<sup>-1</sup>),<sup>16</sup> more HO<sup>•</sup> and Cl<sup>•</sup> were formed at lower pH. On the other hand, the scavenging effects of HO<sup>•</sup> and Cl<sup>•</sup> by OCl<sup>-</sup> are higher than that by HOCl, and the scavenging reactions form ClO<sup>•</sup> (as shown in eqn (6)–(9)). Thus,  $k'_{\text{HO}^{\bullet}}$  decreased significantly while  $k'_{\text{RCS}}$  varied slightly in the UV/chlorine AOP with the increase of the pH value.

**3.2.3. Effect of oxidant dosage on the kinetics and radical contribution.** Fig. 4 shows the  $k'$  of UV, oxidants, HO<sup>•</sup> and RCS for NPX degradation by the UV/chlorine and UV/H<sub>2</sub>O<sub>2</sub> AOPs at pH 7 with increasing chlorine dosage from 0 to 200 μM, respectively. The NPX degradation by UV/chlorine was much more effective than that by UV/H<sub>2</sub>O<sub>2</sub> AOP at the same oxidant dosages. As the dosages of chlorine and H<sub>2</sub>O<sub>2</sub> increased from 20 μM to 200 μM, the  $k'$  of UV/chlorine and UV/H<sub>2</sub>O<sub>2</sub> increased linearly ( $R^2 = 0.998$ ). However, the increase in the  $k'$  of specific radicals with increasing oxidant dosage showed different trends for the two AOPs. The  $k'_{\text{HO}^{\bullet}}$  increased linearly with increasing H<sub>2</sub>O<sub>2</sub> dosage in the UV/H<sub>2</sub>O<sub>2</sub>, while the increase of  $k'_{\text{HO}^{\bullet}}$  slowed down in the UV/chlorine. Meanwhile, the linear increase of total  $k'$  by UV/chlorine is attributable to the increased  $k'_{\text{RCS}}$  proportion from 58.5% to

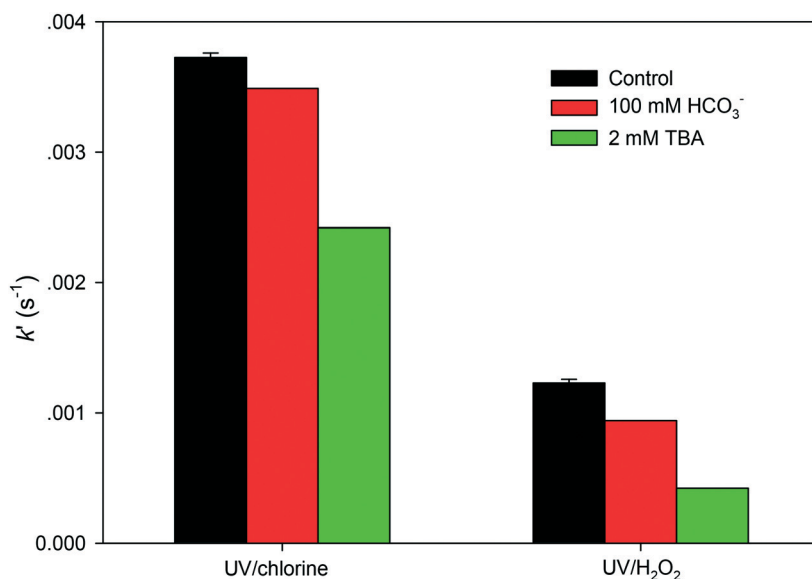


Fig. 3  $k'$  of NPX degradation by the UV/chlorine and UV/H<sub>2</sub>O<sub>2</sub> AOPs in the presence of different radical scavengers at pH 8.4. Conditions: [NPX]<sub>0</sub> = 5 μM, [chlorine]<sub>0</sub> = [H<sub>2</sub>O<sub>2</sub>]<sub>0</sub> = 50 μM, [HCO<sub>3</sub><sup>-</sup>]<sub>0</sub> = 100 mM, [TBA]<sub>0</sub> = 2 mM, [phosphate buffer]<sub>0</sub> = 2 mM.

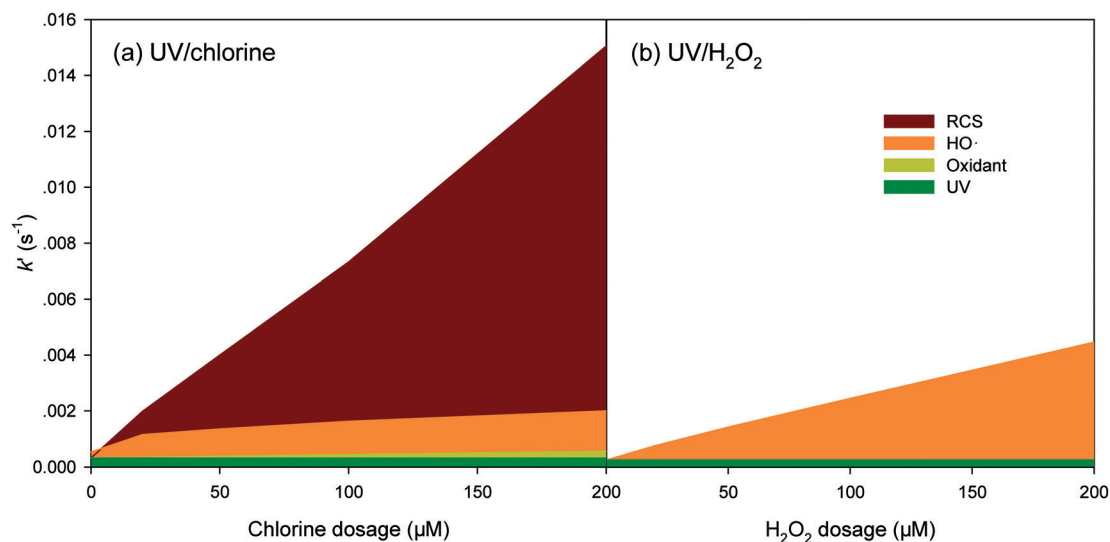


Fig. 4 Effect of oxidant dosage on the  $k'$  of NPX degradation by UV irradiation, oxidant,  $\text{HO}\cdot$ , and RCS ( $\text{Cl}\cdot$ ,  $\text{ClO}\cdot$ ,  $\text{Cl}_2\cdot^-$ ) in the UV/chlorine and UV/ $\text{H}_2\text{O}_2$  AOPs at pH 7. Conditions:  $[\text{chlorine}]_0 = [\text{H}_2\text{O}_2]_0 = 20\text{--}200\ \mu\text{M}$ ,  $[\text{NPX}]_0 = 5\ \mu\text{M}$ ,  $[\text{NB}]_0 = 1\ \mu\text{M}$ ,  $[\text{phosphate buffer}]_0 = 2\ \text{mM}$ .

90.6% with increasing chlorine dosage from 20  $\mu\text{M}$  to 200  $\mu\text{M}$ . These data are consistent with the case of trimethoprim degradation by UV/chlorine, in which  $\text{ClO}\cdot$  generated from the scavenging of  $\text{HO}\cdot$  and  $\text{Cl}\cdot$  by  $\text{HOCl}/\text{OCl}^-$  could attack the methoxyl group on trimethoprim<sup>22</sup> and dimethoxybenzenes.<sup>40</sup> The similar phenomenon suggests that NPX degradation can also be attributable to  $\text{ClO}\cdot$  due to a methoxyl group on the naphthalene ring of NPX.

To further confirm the role of  $\text{ClO}\cdot$  in the degradation of NPX by UV/chlorine, the second-order rate constant of  $\text{ClO}\cdot$  and NPX was investigated.<sup>24</sup> Fig. S4† shows the competition kinetics of NPX *versus* DMOB by  $\text{ClO}\cdot$ . The second-order rate constant of  $\text{ClO}\cdot$  reacting with NPX was determined to be  $<5.69 (\pm 0.36) \times 10^9\ \text{M}^{-1}\ \text{s}^{-1}$ . Note that because  $\text{CO}_3\cdot^-$  was also

involved in the system,<sup>22</sup> this determined rate constant was attributable to both  $\text{ClO}\cdot$  and  $\text{CO}_3\cdot^-$ . The role of  $\text{CO}_3\cdot^-$  could not be neglected, as the rate constant of  $\text{CO}_3\cdot^-$  reacting with NPX was reported to be  $5.6 \times 10^7\ \text{M}^{-1}\ \text{s}^{-1}$ .<sup>13</sup>

### 3.3. Effects of water matrix in simulated water and real water

Fig. 5 shows the  $k'$  of NPX in the UV/chlorine and UV/ $\text{H}_2\text{O}_2$  AOPs in the presence of a variety of water matrix components such as natural organic matter (NOM), bromide ( $\text{Br}^-$ ), chloride ( $\text{Cl}^-$ ), ammonium ( $\text{NH}_4^+$ ) and bicarbonate ion ( $\text{HCO}_3^-$ ).

**3.3.1. Effect of NOM.** NOM retarded NPX degradation in both AOPs. As the concentration of NOM increased from 0 to 3  $\text{mg L}^{-1}$ ,  $k'$  decreased from  $1.44 \times 10^{-3}\ \text{s}^{-1}$  to  $6.9 \times 10^{-4}\ \text{s}^{-1}$  in

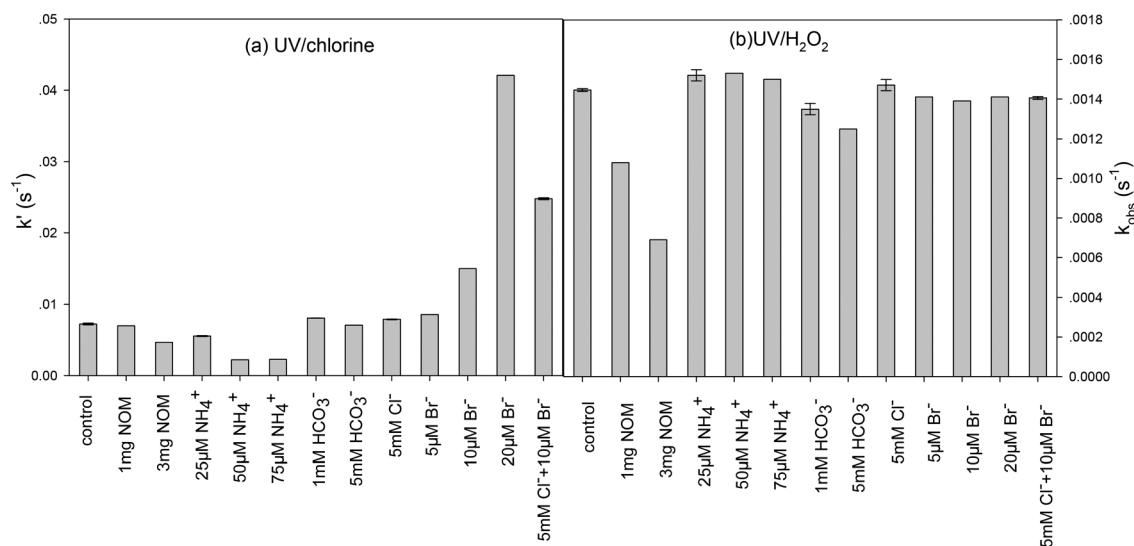
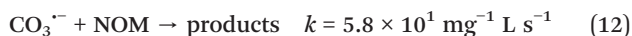
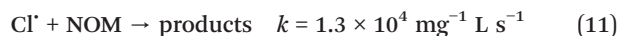
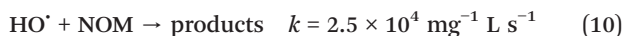
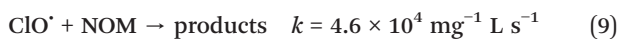


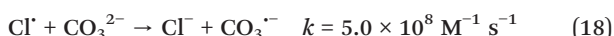
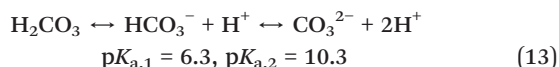
Fig. 5 Effects of water matrix components on the  $k'$  of NPX degradation by UV/chlorine (a) and UV/ $\text{H}_2\text{O}_2$  (b) AOPs in pure water at pH 7. Conditions:  $[\text{chlorine}]_0 = [\text{H}_2\text{O}_2]_0 = 50\ \mu\text{M}$ ,  $[\text{NPX}]_0 = 5\ \mu\text{M}$ ,  $[\text{phosphate buffer}]_0 = 2\ \text{mM}$ .

UV/H<sub>2</sub>O<sub>2</sub> and from  $7.25 \times 10^{-3} \text{ s}^{-1}$  to  $4.69 \times 10^{-3} \text{ s}^{-1}$  in UV/chlorine. NOM inhibited the degradation in two ways: (1) NOM acted as an inner filter of UV light to reduce the production of radicals of HO<sup>•</sup> and/or RCS; (2) NOM competed with NPX to consume HO<sup>•</sup> and RCS (eqn (9)–(12)).<sup>16,23,24</sup>



The molar absorption coefficient ( $\epsilon_{254 \text{ nm}}$ ) of NOM was  $3.15 \text{ mg}^{-1} \text{ L m}^{-1}$ ;<sup>16</sup> 1 and 3 mg L<sup>-1</sup> NOM filtered 8.1% and 29.9% UV light, respectively, in the UV/chlorine and UV/H<sub>2</sub>O<sub>2</sub> AOPs. However, in the presence of 3 mg L<sup>-1</sup> NOM, the overall  $k$ 's were inhibited by 35% and 52% in UV/chlorine and UV/H<sub>2</sub>O<sub>2</sub>, respectively. This results indicated that the inner filter effect by NOM was the primary reason in UV/chlorine, while radical scavenging by NOM was the primary reason in UV/H<sub>2</sub>O<sub>2</sub>. However, the inhibition of  $k$  by UV/chlorine was lower than that by UV/H<sub>2</sub>O<sub>2</sub>, which could be attributable to the non-selective HO<sup>•</sup> being more susceptible than the selective RCS.

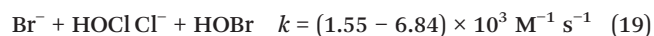
**3.3.2. Effect of bicarbonate.** HCO<sub>3</sub><sup>-</sup>, a common ion present in real water, reacts with HO<sup>•</sup>, Cl<sup>•</sup> and Cl<sub>2</sub><sup>-•</sup> in the systems and transforms into CO<sub>3</sub><sup>-•</sup> (eqn (13)–(18)).<sup>16,22</sup>



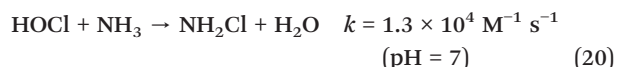
However, the presence of HCO<sub>3</sub><sup>-</sup> did not decrease the NPX degradation efficiency of both AOPs, which is not consistent with the previous studies. For example, ibuprofen degradation by UV/chlorine<sup>20</sup> and phenol degradation by UV/H<sub>2</sub>O<sub>2</sub> (ref. 25) were reduced by the presence of HCO<sub>3</sub><sup>-</sup>. CO<sub>3</sub><sup>-•</sup> ( $E^{\circ}(\text{CO}_3^{\bullet -}/\text{CO}_3^{2-}) = 1.63 \text{ V}$  at pH 8.4) is effective to degrade oxytetracycline, trimethoprim, sulfamethoxazole *etc.*<sup>41,42</sup> The second-order rate constant for CO<sub>3</sub><sup>-•</sup> reacting with NPX has been reported to be  $5.6 \times 10^7 \text{ M}^{-1} \text{ s}^{-1}$ ,<sup>13</sup> thus the contribution of CO<sub>3</sub><sup>-•</sup> to NPX degradation could not be neglected. According to the simulated kinetics model, the increase of  $k'_{\text{CO}_3^{\bullet -}}$  (*i.e.*  $k'_{\text{NPX-CO}_3^{\bullet -}}[\text{CO}_3^{\bullet -}]$ ) is comparable with the loss of  $k'_{\text{HO}^{\bullet}}$  (*i.e.*

$k'_{\text{NPX-HO}^{\bullet}}[\text{HO}^{\bullet}]$ ) with the addition of HCO<sub>3</sub><sup>-</sup> in UV/chlorine and UV/H<sub>2</sub>O<sub>2</sub> (Table S3<sup>†</sup>). Thus, CO<sub>3</sub><sup>-•</sup> contributed to the NPX degradation to compensate for the loss of HO<sup>•</sup>.

**3.3.3. Effect of halides.** Halides such as Cl<sup>-</sup> and Br<sup>-</sup> are commonly present in real waters. Cl<sup>-</sup> reacts with Cl<sup>•</sup> and HO<sup>•</sup> to form Cl<sub>2</sub><sup>-•</sup> and ClOH<sup>-•</sup>, respectively, and the reactions are reversible (eqn (3)–(5)). The presence of 5 mM Cl<sup>-</sup> would increase the concentration of Cl<sub>2</sub><sup>-•</sup> by 2 orders of magnitude;<sup>16</sup> however, it did not affect the NPX degradation efficiency by both AOPs. This result indicates the low reactivity between NPX and Cl<sub>2</sub><sup>-•</sup>. For Br<sup>-</sup>, Br<sup>-</sup> at the concentration of 5–20 μM has little influence on the  $k'$  by UV/H<sub>2</sub>O<sub>2</sub>, whereas for 20 μM Br<sup>-</sup> in UV/chlorine, the  $k'$  increased more than 3 times. The co-presence of Cl<sup>-</sup> and Br<sup>-</sup> further increased the  $k'$  in UV/chlorine, *i.e.*,  $k'$  was 66.0% higher at 5 mM Cl<sup>-</sup> + 10 μM Br<sup>-</sup> (0.025 s<sup>-1</sup>) compared to that at 10 μM Br<sup>-</sup> (0.015 s<sup>-1</sup>). Additionally, in dark halogenation, the  $k'$  increased significantly in Cl<sup>-</sup> in the presence of Br<sup>-</sup>, and the  $k'$  by dark halogenation (Fig. S5<sup>†</sup>) was 72.7% higher at 5 mM Cl<sup>-</sup> + 10 μM Br<sup>-</sup> (0.019 s<sup>-1</sup>) compared to that at 10 μM Br<sup>-</sup> (0.011 s<sup>-1</sup>). The dramatic increase of  $k'$  in UV/chlorine and dark halogenation can be attributable to the production of HOBr (eqn (19)), with a second-order rate constant with NPX of  $25 \pm 1 \text{ M}^{-1} \text{ s}^{-1}$  (ref. 43) at pH 7 and 20 °C. The dramatic increase of  $k'$  in the co-presence of Cl<sup>-</sup> and Br<sup>-</sup> compared to that in only Br<sup>-</sup> can be responsible for the additional formation of BrCl, which rapidly reacts with organic compounds containing a conjugation ring.<sup>23</sup> In the presence of Br<sup>-</sup>, bromine-containing radicals such as Br<sup>•</sup>, Br<sub>2</sub><sup>-•</sup>, BrO<sup>•</sup> and ClBr<sup>-•</sup> can also contribute to the degradation of NPX in UV/chlorine.<sup>23</sup>



**3.3.4. Effect of ammonia.** The presence of NH<sub>4</sub><sup>+</sup>/NH<sub>3</sub> did not affect  $k'$  of NPX degradation by UV/H<sub>2</sub>O<sub>2</sub>, but it strongly decreased  $k'$  by UV/chlorine. With increasing NH<sub>4</sub><sup>+</sup> concentration from 25 μM to 50 μM, the  $k'$  by UV/chlorine decreased from  $5.55 \times 10^{-3}$  to  $2.22 \times 10^{-3} \text{ M}^{-1} \text{ s}^{-1}$ . This was mainly attributable to the decreased contribution of ClO<sup>•</sup> to NPX degradation. NH<sub>3</sub> consumed HOCl rapidly to form monochloramine at pH 7 (eqn (20)),<sup>44</sup> and ClO<sup>•</sup> was only generated in UV/chlorine as opposed to UV/monochloramine. A previous study also reported that the concentration of ClO<sup>•</sup> decreased as the NH<sub>4</sub><sup>+</sup> to HOCl ratio increased from 0 to 1.<sup>23</sup> The effect of 50 μM and 75 μM NH<sub>4</sub><sup>+</sup> on the UV/chlorine AOP was similar, which was due to chlorine being totally transformed to monochloramine when NH<sub>4</sub><sup>+</sup> ≥ 50 μM (ammonia: chlorine ≥ 1).



**3.3.5. Effect of real water matrix.** Fig. 6 compares the  $k'$  of NPX by the UV/chlorine and the UV/H<sub>2</sub>O<sub>2</sub> AOPs in ultrapure water and a tap water sample from Nanzhou water treatment plant in Guangzhou, China. The concentrations of

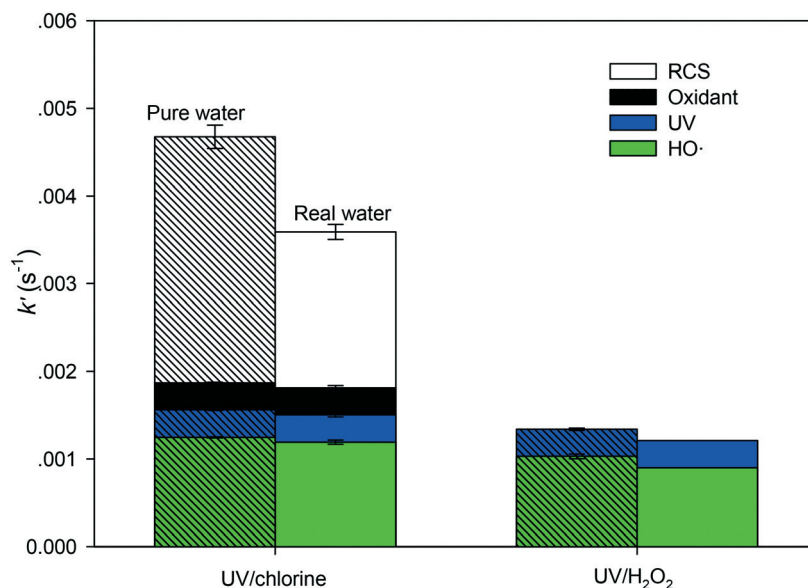


Fig. 6 Comparison of  $k'$  of NPX degradation by UV irradiation, chlorination,  $\text{HO}\cdot$ , and RCS ( $\text{Cl}\cdot$ ,  $\text{ClO}\cdot$ ,  $\text{Cl}_2\cdot^-$ ) in the UV/chlorine and UV/ $\text{H}_2\text{O}_2$  AOPs in pure water and real water at pH 7. Conditions:  $[\text{chlorine}]_0 = [\text{H}_2\text{O}_2]_0 = 50 \mu\text{M}$ ,  $[\text{NPX}]_0 = 5 \mu\text{M}$ ,  $[\text{NB}]_0 = 1 \mu\text{M}$ ,  $[\text{phosphate buffer}]_0 = 2 \text{mM}$ .

ammonium, chloride, bicarbonate and DOC in the real water sample were  $0.04 \text{ mg L}^{-1}$  (as N),  $16.03 \text{ mg L}^{-1}$ ,  $58.56 \text{ mg L}^{-1}$  (as  $\text{HCO}_3^-$ ) and  $0.628 \text{ mg L}^{-1}$ , respectively. The concentration of bromide was undetectable (Table S4†). In the UV/chlorine and UV/ $\text{H}_2\text{O}_2$  AOPs, for the real water compared to pure water, the  $k'$  decreased by 23.2% and 9%, respectively. The  $k'_{\text{HO}\cdot}$  and  $k'_{\text{RCS}}$  by UV/chlorine decreased by 4.5% and 29.7%, respectively. As discussed above, the existence of ammonium and NOM in the real water can be primarily attributable to the significantly reduced  $k'_{\text{RCS}}$  in UV/chlorine compared to pure water. Nevertheless, the degradation efficiency of NPX

in real water was still much higher by UV/chlorine than by UV/ $\text{H}_2\text{O}_2$ .

### 3.4. Degradation pathways

The total ion chromatograms of UPLC-QTOF MS of the samples during the NPX degradation by UV/ $\text{H}_2\text{O}_2$  and UV/chlorine are shown in Fig. S6†. Based on the accurate mass-to-charge ratios ( $m/z$ ) provided by TOFMS, the proposed formulas of products were provided (Table S5†). Isomers were differentiated by different LC retention time. The structures of these products were further confirmed by MS and MS2 fragmentation using Q-TOFMS and are listed in Table S6 and Fig.

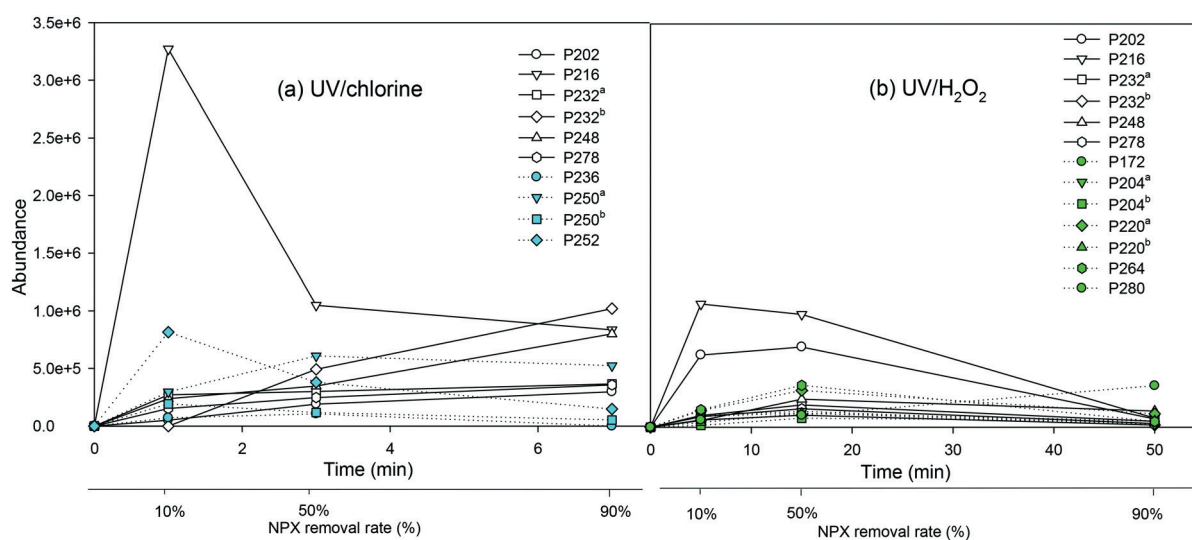


Fig. 7 Evolution of transformation products with the reaction time in (a) the UV/chlorine and (b) UV/ $\text{H}_2\text{O}_2$  AOPs. Blue, green and hollow symbols show the products generated in UV/chlorine only, in UV/ $\text{H}_2\text{O}_2$  only and common products in both AOPs, respectively. Conditions:  $[\text{chlorine}]_0 = [\text{H}_2\text{O}_2]_0 = 200 \mu\text{M}$ ,  $[\text{NPX}]_0 = 50 \mu\text{M}$ ,  $[\text{phosphate buffer}]_0 = 2 \text{mM}$ .

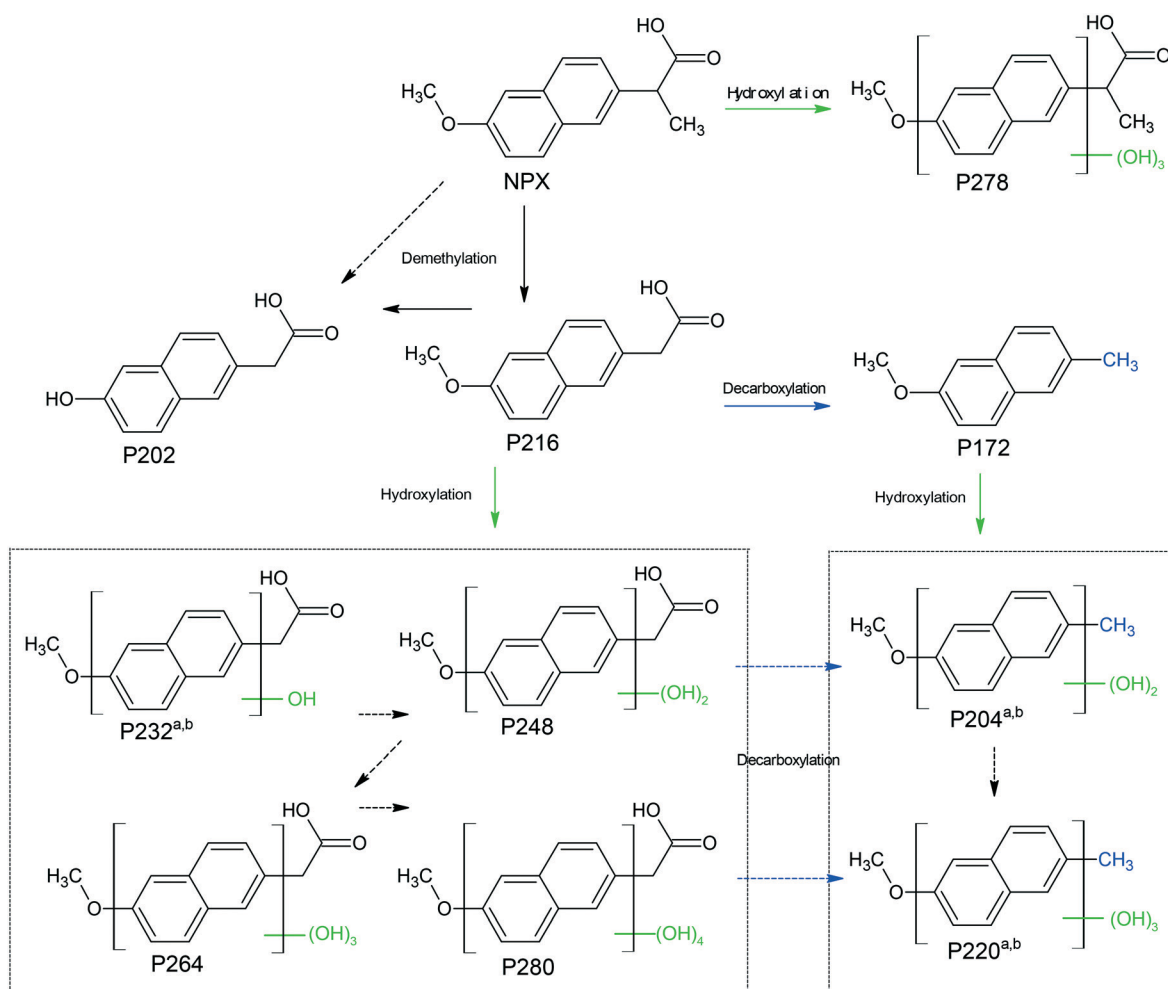
S7.† Fig. 7 compares the evolution of the transformation products by UV/chlorine and UV/H<sub>2</sub>O<sub>2</sub> at the same removal rate of NPX. P202 (C<sub>12</sub>H<sub>10</sub>O<sub>3</sub>, *m/z* 201), P216 (C<sub>13</sub>H<sub>12</sub>O<sub>3</sub>, *m/z* 215), P232<sup>a,b</sup> (C<sub>13</sub>H<sub>12</sub>O<sub>4</sub>, *m/z* 231), P248 (C<sub>13</sub>H<sub>12</sub>O<sub>5</sub>, *m/z* 247) and P278 (C<sub>14</sub>H<sub>14</sub>O<sub>6</sub>, *m/z* 277) were observed in both AOPs. P236 (C<sub>12</sub>H<sub>8</sub>O<sub>3</sub>Cl, *m/z* 235), P250<sup>a,b</sup> (C<sub>13</sub>H<sub>11</sub>O<sub>3</sub>Cl, *m/z* 249) and P252 (C<sub>12</sub>H<sub>9</sub>O<sub>4</sub>Cl, *m/z* 251) and were observed only in UV/chlorine. P172 (C<sub>12</sub>H<sub>12</sub>O, *m/z* 171), P204<sup>a,b</sup> (C<sub>12</sub>H<sub>12</sub>O<sub>3</sub>, *m/z* 203), P220<sup>a,b</sup> (C<sub>12</sub>H<sub>12</sub>O<sub>4</sub>, *m/z* 219), P264 (C<sub>13</sub>H<sub>12</sub>O<sub>6</sub>, *m/z* 263) and P280 (C<sub>13</sub>H<sub>12</sub>O<sub>7</sub>, *m/z* 279) were observed only in UV/H<sub>2</sub>O<sub>2</sub>. The abundance of P216 was the highest in both AOPs.

In general, an initially increased and then decreased trend was observed for most products, indicating the further degradation of these products by radical attack and/or UV photolysis during the two AOPs. The peaked abundances of the common products in both AOPs were higher in UV/chlorine than in UV/H<sub>2</sub>O<sub>2</sub> (Fig. 7). For example, the major product P216 with the highest abundance in both AOPs peaked at 1 min and then decreased by 68% from 1 min to 3 min (from 10% to 50% removal rate of NPX) in UV/chlorine; the abundance of P216 was  $3.27 \times 10^6$  at 1 min, which decreased to  $1.05 \times 10^6$  at 3 min, while it peaked at 5 min and then gradually de-

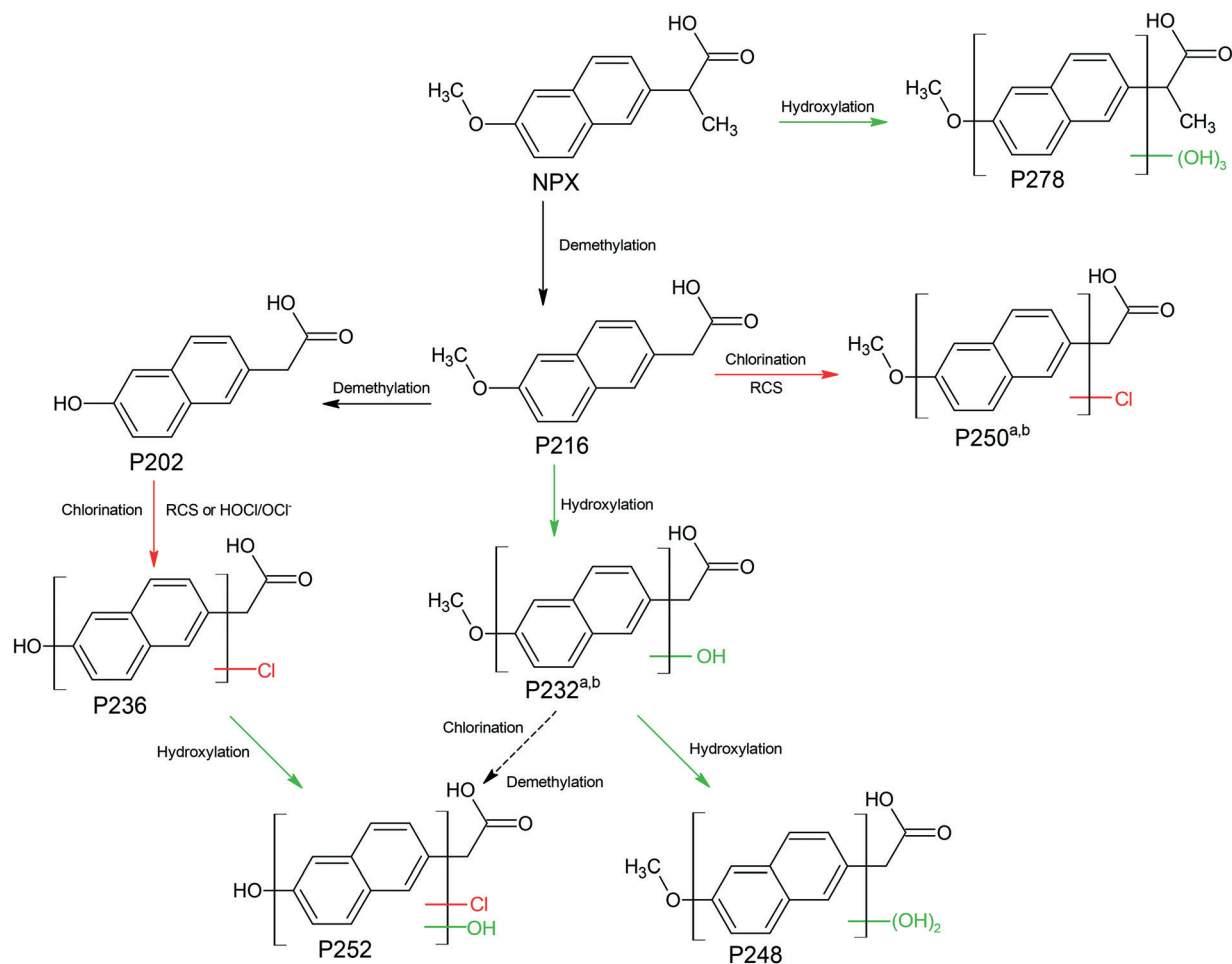
creased from 5 to 15 min (from 10% to 50% removal rate of NPX) in UV/H<sub>2</sub>O<sub>2</sub>. The peaked abundance of P216 was 3.1 times higher in UV/chlorine than that in UV/H<sub>2</sub>O<sub>2</sub>. This result could be attributable to the higher reactivity of RCS to form P216 than HO<sup>•</sup>. Meanwhile, P216 contains a methoxyl group, which could be rapidly attacked by ClO<sup>•</sup>;<sup>22</sup> thus it also decreased faster in UV/chlorine than in UV/H<sub>2</sub>O<sub>2</sub>. Based on the identified products and their evolution, the degradation pathways of NPX by the UV/H<sub>2</sub>O<sub>2</sub> and UV/chlorine AOPs are proposed in Schemes 1 and 2, respectively.

In the UV/H<sub>2</sub>O<sub>2</sub> AOP, at the beginning of the NPX degradation, demethylation and hydroxylation were observed as two major pathways which produced P216 and P278, respectively. Then, demethylation and decarboxylation of P216 were observed to form P202 and P172. Through further oxidation by HO<sup>•</sup>, P216 generated a series of hydroxylation products such as P232<sup>a,b</sup>, P248, P264 and P280. P204<sup>a,b</sup> and P220<sup>a,b</sup> were formed by either hydroxylation of P172 or decarboxylation of P248 and P264. Hydroxylation and decarboxylation were also observed in the ibuprofen degradation in the UV/H<sub>2</sub>O<sub>2</sub> AOP.<sup>45</sup>

In the UV/chlorine AOP, the first step was similar to UV/H<sub>2</sub>O<sub>2</sub>, which formed P216 and P278 by demethylation and



Scheme 1 Proposed pathways of the NPX degradation by the UV/H<sub>2</sub>O<sub>2</sub> AOP.



Scheme 2 Proposed pathways of the NPX degradation by the UV/chlorine AOP.

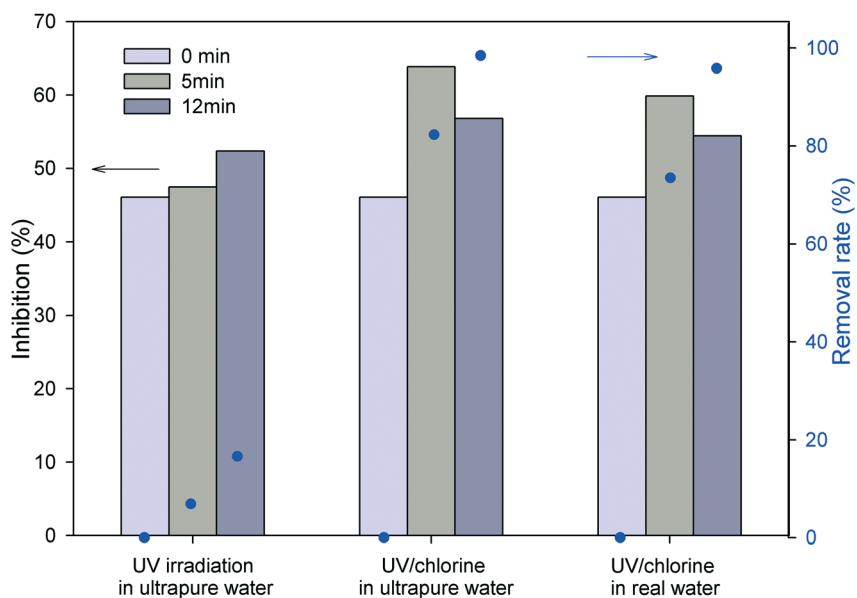


Fig. 8 Alternation of acute toxicity (inhibition of *Vibrio fischeri*) at different reaction times in direct UV photolysis and the UV/chlorine AOP at pH 7. Bars show the acute toxicities and blue symbols show the removal rates of NPX. Conditions:  $[\text{chlorine}]_0 = 50 \mu\text{M}$ ,  $[\text{NPX}]_0 = 5 \mu\text{M}$ .

hydroxylation, respectively. The involvement of RCS and HOCl/OCl<sup>-</sup> results in chlorine-containing products. The reactions of P216 with RCS generated two monochlorinated isomers P250<sup>a,b</sup>. The demethylation of P216 formed P202, which can react with RCS and/or HOCl/OCl<sup>-</sup> to generate P236. P216 could also undergo hydroxylation to generate P232<sup>a,b</sup> and P248. However, their further hydroxylation products with more hydroxyl groups such as P264 and P280, identified in the UV/H<sub>2</sub>O<sub>2</sub> AOP, were not observed. P252 containing both chlorine and hydroxyl group was generated by either hydroxylation of P236 or the simultaneous chlorination and demethylation of P232<sup>a,b</sup>.

### 3.5. Toxicity alternation

Fig. 8 shows the acute toxicity alternation during NPX degradation by UV photolysis and the UV/chlorine AOP at different reaction times in pure water and real water. For the samples treated by UV, the inhibition (%) of *Vibrio fischeri* increased from 46.1% to 52.3%. This result was consistent with a previous study which shows that UV irradiation increased the toxicity of NPX.<sup>46</sup> The inhibition peaked at 5 min (63.8%) but decreased to 56.8% at 12 min for the samples treated by UV/chlorine in pure water. The acute toxicity for the samples treated by UV/chlorine was slightly lower in real water than in pure water. The toxicity alternation was consistent with the variation of the products such as P216 and P252 in the UV/chlorine AOP (Fig. 7), indicating that the products may be associated with the toxicity alternation.

## 4. Conclusions

The efficiency of NPX degradation by UV/chlorine was much higher than that of UV/H<sub>2</sub>O<sub>2</sub> under all the tested conditions such as different pHs (6–9), different oxidant dosages, different water matrix of NOM, bicarbonate, halides and ammonia, and in a real water sample.

RCS such as Cl<sup>•</sup> and ClO<sup>•</sup> played dominant roles in the NPX degradation by UV/chlorine at pH 6–9, particularly at higher pH. The second-order rate constant of ClO<sup>•</sup> with NPX was determined to be  $<5.69 (\pm 0.36) \times 10^9 \text{ M}^{-1} \text{ s}^{-1}$ .

The degradation by both AOPs was associated with hydroxylation and demethylation; in particular, decarboxylation was observed in UV/H<sub>2</sub>O<sub>2</sub> and chlorine substitution was observed in UV/chlorine. The acute toxicity to *Vibrio fischeri* in UV/chlorine followed an increase and then a decrease trend with increasing reaction time.

This study comprehensively compared the degradation of NPX by the UV/chlorine and UV/H<sub>2</sub>O<sub>2</sub> AOPs. The much better efficiency of the UV/chlorine AOP compared to the UV/H<sub>2</sub>O<sub>2</sub> AOP indicates that the former can be a good alternative to the latter for the degradation of micropollutants.

## Conflicts of interest

There are no conflicts to declare.

## Acknowledgements

This work was financially supported by the Natural Science Foundation of China (21677181), the National Key Research Development Program of China (2016YFC0502803), the Top-Top Scientific and Technical Innovative Youth Talents of Guangdong Special Support Program (2015TQ01Z552), the Science and Technology Project of Zhejiang Province (Grant No. 2017C33036), the Guangzhou Science Technology and Innovation Commission (201707010249), and the Fundamental Research Funds for the Central Universities (17lgzd21).

## References

- 1 M. J. Benotti, R. A. Trenholm, B. J. Vanderford, J. C. Holady, B. D. Stanford and S. A. Snyder, *Environ. Sci. Technol.*, 2009, **43**, 597–603.
- 2 B. Kasprzyk-Hordern, R. M. Dinsdale and A. J. Guwy, *Water Res.*, 2008, **42**, 3498–3518.
- 3 O. Frédéric and P. Yves, *Chemosphere*, 2014, **115**, 31–39.
- 4 J. Jensen and J. J. Scott-Fordsmand, *Environ. Pollut.*, 2012, **171**, 133–139.
- 5 J. C. Durán-Álvarez, B. Prado, D. González, Y. Sánchez and B. Jiménez-Cisneros, *Sci. Total Environ.*, 2015, **538**, 350–362.
- 6 M. Klavarioti, D. Mantzavinos and D. Kassinos, *Environ. Int.*, 2009, **35**, 402–417.
- 7 X. Peng, W. Ou, C. Wang, Z. Wang, Q. Huang, J. Jin and J. Tan, *Sci. Total Environ.*, 2014, **490**, 889–898.
- 8 G. R. Boyd, S. Zhang and D. A. Grimm, *Water Res.*, 2005, **39**, 668–676.
- 9 Z. Wang, X. Zhang, Y. Huang and H. Wang, *Environ. Pollut.*, 2015, 223–232.
- 10 E. Carmona, V. Andreu and Y. Picó, *Sci. Total Environ.*, 2014, **484**, 53–63.
- 11 N. Nakada, T. Tanishima, H. Shinohara, K. Kiri and H. Takada, *Water Res.*, 2006, **40**, 3297–3303.
- 12 S. C. Paul, L. J. M. Githinji, R. O. Ankumah, K. R. Willian and G. Pritchett, *Water, Air, Soil Pollut.*, 2014, **225**, 1821.
- 13 B. A. Wols, D. J. Harmsen, J. Wandersdijk, E. F. Beerendonk and C. H. Hofmancaris, *Water Res.*, 2015, **75**, 11–24.
- 14 S. B. Abdelmelek, J. Greaves, K. P. Ishida, W. J. Cooper and W. Song, *Environ. Sci. Technol.*, 2011, **45**, 3665–3671.
- 15 I. A. Katsoyiannis, S. Canonica and U. von Gunten, *Water Res.*, 2011, **45**, 3811–3822.
- 16 J. Fang, Y. Fu and C. Shang, *Environ. Sci. Technol.*, 2014, **48**, 1859–1868.
- 17 C. Sichel, C. Garcia and K. Andre, *Water Res.*, 2011, **45**, 6371–6380.
- 18 M. J. Watts, *J. Water Supply: Res. Technol.-AQUA*, 2007, **56**, 469–477.
- 19 P. Sun, W. N. Lee, R. Zhang and C. H. Huang, *Environ. Sci. Technol.*, 2016, **50**, 13265–13273.
- 20 Y. Xiang, J. Fang and C. Shang, *Water Res.*, 2016, **90**, 301–308.

- 21 J. Zhao, G. Ying, L. Wang, J. Yang, X. Yang, L. Yang and X. Li, *Sci. Total Environ.*, 2009, **407**, 962–974.
- 22 Z. Wu, J. Fang, Y. Xiang, C. Shang, X. Li, F. Meng and X. Yang, *Water Res.*, 2016, **104**, 272–282.
- 23 Z. Wu, K. Guo, J. Fang, X. Yang and H. Xiao, *Water Res.*, 2017, **126**, 351.
- 24 K. Guo, Z. Wu, C. Shang, B. Yao and S. Hou, *Environ. Sci. Technol.*, 2017, **51**, 10431.
- 25 J. E. Grebel, J. J. Pignatello and W. A. Mitch, *Environ. Sci. Technol.*, 2010, **44**, 6822–6828.
- 26 Y. H. Chuang, S. Chen, C. Chinn and W. A. Mitch, *Environ. Sci. Technol.*, 2017, **51**, 13859–13868.
- 27 X. Yang, J. Sun, W. Fu, C. Shang, Y. Li, Y. Chen, W. Gan and J. Fang, *Water Res.*, 2016, **98**, 309–318.
- 28 S. W. Nam, Y. Yoon, D. J. Choi and K. D. Zoh, *J. Hazard. Mater.*, 2015, **285**, 453–463.
- 29 S. Zhou, Y. Xia, T. Li, T. Yao, Z. Shi, S. Zhu and N. Gao, *Environ. Sci. Pollut. Res.*, 2016, **23**, 16448–16455.
- 30 Y. Li, W. Song, W. Fu, D. C. W. Tsang and X. Yang, *Chem. Eng. J.*, 2015, **271**, 214–222.
- 31 APHA-AWWA-WEF, *Standard Methods for the Examination of Water and Wastewater*, Washington DC, 2012.
- 32 N. V. Klassen, D. Marchington and H. C. E. McGowan, *Anal. Chem.*, 1994, **66**, 2921–2925.
- 33 J. R. Bolton, M. I. Stefan, P. Shaw and K. R. Lykke, *J. Photochem. Photobiol., A*, 2011, **222**, 166–169.
- 34 T. Garoma and M. D. Gurol, *Environ. Sci. Technol.*, 2005, **39**, 7964–7969.
- 35 B. A. Wols, C. H. M. Hofman-Caris, D. J. H. Harmsen and E. F. Beerendonk, *Water Res.*, 2013, **47**, 5876–5888.
- 36 E. Arany, R. K. Szabó, L. Apáti, T. Alapi, I. Ilisz, P. Mazellier, A. Dombi and K. Gajda-Schranz, *J. Hazard. Mater.*, 2013, **262**, 151–157.
- 37 Y. Feng, D. W. Smith and J. R. Bolton, *J. Environ. Eng. Sci.*, 2007, **6**, 277–284.
- 38 S. M. Alpert, D. R. Knappe and J. J. Ducoste, *Water Res.*, 2010, **44**, 1797–1808.
- 39 The Radiation Chemistry Data Center of the Notre Dame Radiation Laboratory (ndrlrCDC), *Kinetics Database*, <http://www3.nd.edu/~ndrlrCDC/index.html>.
- 40 Z. B. Alfassi, R. E. Huie, S. Mosseri and P. Neta, *Radiat. Phys. Chem.*, 1988, **32**, 3888–3891.
- 41 Y. Liu, X. He, X. Duan, Y. Fu and D. D. Dionysiou, *Chem. Eng. J.*, 2015, **276**, 113–121.
- 42 R. Zhang, Y. Yang, C. Huang, N. Li, H. Liu, L. Zhao and P. Sun, *Environ. Sci. Technol.*, 2016, **50**, 2573–2583.
- 43 M. B. Heeb, J. Criquet, S. G. Zimmermann-Steffens and U. von Gunten, *Water Res.*, 2014, **48**, 15–42.
- 44 M. Deborde and U. von Gunten, *Water Res.*, 2008, **42**, 13–51.
- 45 M. Peng, H. Li, X. Kang, E. Du and D. Li, *Water Sci. Technol.*, 2017, **75**, 2935.
- 46 M. Isidori, M. Lavorgna, A. Nardelli, A. Parrella, L. Previtiera and M. Rubino, *Sci. Total Environ.*, 2005, **348**, 93–101.